RESEARCH ARTICLE

A toolbox to explore the composition of species dynamics behind multi-species indices

Stanislas Rigal | **Jonas Knape**

Department of Ecology, Swedish University of Agricultural Sciences, Uppsala, Sweden

Correspondence
Stanislas Rigal
Email: stanislas.rigal@ens-lyon.fr

Funding information
Svenska Forskningsrådet Formas, Grant/Award Number: 2017-1064

Handling Editor: Res Altwegg

Abstract

1. In the light of declining biodiversity, monitoring its fate is essential for conservation strategies. Aggregation of temporal change of different species into multi-species indices such as geometric means makes it possible to identify species groups that are at risk as well as those that are doing well. However, aggregated indices mask the between-species variability in the temporal trajectories, which could be of high relevance for conservation actions.

2. We propose a toolbox, available as an R package, to investigate compositions of species dynamics in geometric mean multi-species indices. The toolbox is based on a dynamic factor analysis which uses species dynamics and their uncertainty to (1) identify common latent trends in those species dynamics, (2) display the variability of species dynamics and (3) extract clusters of species with similar dynamics within the species groups used for the indices.

3. We apply the toolbox to common breeding birds in Sweden and explore the variability in dynamics among species included in EU-official indices for farmland and woodland species, highlighting clusters of species with related dynamics previously hidden by averaging.

4. The toolbox is designed to be applicable to a wide range of ecological monitoring data. By enabling a deeper exploration of the structure behind existing indices, we may refine our understanding of biodiversity change to better inform subsequent conservation policies.

KEYWORDS
biodiversity index, DFACLUST R package, dynamic factor analysis, species clustering, species dynamics variability

1 | INTRODUCTION

Monitoring populations is crucial for tracking ongoing changes in biodiversity (Keith et al., 2015) and progress towards conservation targets (Costelloe et al., 2016). A common approach to assess biodiversity change is to compute biodiversity indicators across a group of species (e.g. the Living Planet Index; Loh et al., 2005), such as the change in geometric mean of relative abundances of a set of species (Buckland et al., 2005) (e.g. the Grassland Butterfly Indicator (Van Swaay et al., 2019), the Wild Bird Indicator (Gregory & Van Strien, 2010)). These multi-species indices (MSIs) are often

constructed from species that share similar habitats or ecological traits and are then used as proxies to evaluate the status and changes of a given environment, even becoming official indicators (EEA, 2019), particularly because of their simplicity of interpretation. For example, MSIs have been used to sound the alarm about continuing declines of common farmland birds (Freeman et al., 2001; Gregory et al., 2003) and in characterising the onset of recovery of some rarer wetland birds (Inger et al., 2015).

Since aggregated biodiversity indices summarise the main trajectory of a group of species, trajectories of single species are obscured, and these can potentially vary greatly within the species group (Gregory et al., 2007). For instance, a declining MSI trend could emerge from the aggregation of many decreasing populations, or from a few strongly decreasing populations and several stable or moderately increasing ones, the topic of a recent debate concerning interpretation of the Living Planet Index (Leung et al., 2020; Loreau et al., 2022). The trajectory of some species may also be driven by factors that do not affect other species within the index, resulting in different trends for those species compared to others and the aggregated index. There is currently a paucity of formal tools for investigating the structure and diversity among population trajectories in the group of species underlying biodiversity indicators (but see Gaüzère et al., 2019). Available approaches are to examine species-wise slope coefficients (Julliard et al., 2004), or simple sensitivity analyses where the effects of leaving species out in the computation of the index are examined (Leung et al., 2020).

In this study, we use dynamic factor analysis (DFA) (Zuur et al., 2003) in combination with a clustering analysis of DFA output as a tool for exploring structures in species dynamics underlying aggregated geometric mean biodiversity indicators. DFA is a type of multivariate state-space model (Holmes et al., 2012) that represents the main dynamic features of a set of observed time series using a, typically small, number of latent dynamic trajectories while accounting for observation and process error. These latent trends may be interpreted as building blocks for constructing the trends of the species (via linear combinations). DFA can also be thought of as a dimension-reduction technique for time series that may be used to extract shared dynamic features from a set of time series while incorporating the uncertainty of each time series (Zuur et al., 2003). DFA has been mostly used in marine ecology (e.g. to analyse the dynamics of fish stocks (Lin et al., 2021; Zimmermann et al., 2019)), and constitutes a means of relating trajectories of different species to each other by considering how they relate to the latent dynamics of the set of species.

Based on a DFA model, we propose a toolbox, available as an R package, that aims to explore the structure underlying geometric mean biodiversity indices. The toolbox takes time series of species indices and their associated uncertainty as input and provides (1) estimates of latent trends which correspond to the main features of the dynamics among the species, (2) ordination plots visualising the distribution of species dynamics along the latent trends and (3) a clustering of species sharing similar dynamics. This toolbox can reveal important information about the heterogeneity in species

dynamics inside an aggregated species index. We first present the DFA and the three related tools. Then, we apply it to empirical data on Swedish breeding birds and the two main habitat specific multi-species indices, the farmland and woodland bird indicators, which are used as official biodiversity health indicators in Sweden and the European Union (Svensk fågeltaxerings, 2021). Finally, we use simulations to explore the performance of the method.

2 | MATERIALS AND METHODS

2.1 | Time-series analysis

2.1.1 | Dynamic factor analysis

The first step of the toolbox is to fit a DFA model to time series of species-wise population indices and their associated uncertainties. In DFA, the dynamics of a set of time series is described as linear combinations of a smaller number of latent trends (Zuur et al., 2003). These latent trends correspond to unobserved common dynamics (i.e. 'trend' here does not necessarily refer to a linear process) that are used to model the observed species time series. This allows capturing shared features of the dynamics across multiple observed series, which we aim to use to explore structures of dynamics hidden behind population indices. Our DFA for estimated population indices, using M latent trends for I species, may be described as (Equation 1):

$$y_{i,t} = z_{i,1}\alpha_{1,t} + z_{i,2}\alpha_{2,t} + \ldots + z_{i,M}\alpha_{M,t} + \epsilon_{i,t} + \eta_{i,t}. \quad (1)$$

Here, $y_{i,t}$ is the population index for species i at time t, which we will assume to be mean centred at the log scale, the $z_{i,j}$ are factor loadings of species i for the corresponding latent trend j, and $\alpha_{j,t}$ is the value of the common latent trend j at time t (mean-centred to obtain $z_{i,j}$). The noise component consists of two parts, $\eta_{i,t}$ and $\epsilon_{i,t}$ both normally distributed with mean 0. The variance of $\epsilon_{i,t}$ is set equal to the squared standard error of the log-scale and mean-centred population index for species i at time t. Thus, ϵ captures the measurement uncertainty associated with the fact that the $y_{i,t}$ are estimated quantities, the uncertainty of the indices being given as input to the DFA model. The variances of the $\eta_{i,t}$ are free parameters estimated for each species, $\eta_{i,t} \sim N(0, \sigma_i)$, with σ_i the species-specific variance. The $\eta_{i,t}$ therefore capture additional random species-specific discrepancies from the latent trends beyond what is captured by the standard errors of the indices. The standard errors of the indices then become lower bounds for the total uncertainty around the linear combination of latent trends. The $\eta_{i,t}$ can optionally be left out, but then the standard errors of the indices need to capture all deviations between indices and the linear combinations of the latent trends, which can require a large number of latent trends. This would be particularly problematic in cases where index standard errors are small and there is large among year variation in the indices. We include $\eta_{i,t}$ in all analyses in this paper although they may sometimes

give boundary estimates (σ_i close to zero) for some species in which case they have no effect.

We model the dynamics of the latent trend $\alpha_{j,t}$ as independent random walks (Equation 2):

$$\alpha_{i,t} = \alpha_{i,t-1} + \nu_{i,t} \qquad (2)$$

with $\nu_{i,t} \sim N(0, 1)$ and $\alpha_{i,0} = 0$. Random walk dynamics are standard in DFA models, although alternatives such as smoother time-series models are possible (Ward et al., 2022). The variance of the random walk disturbances $\nu_{i,t}$ is set to 1 for identifiability reasons (Harvey, 1990). To match the assumption of log-scale mean-centred observed data, we impose a sum-to-zero constraint on the random walks before they are used with Equation (1) (i.e. we are using $\alpha_{i,t} - \alpha_i$).

2.1.2 | DFA implementation

DFA models are not identifiable unless further constraints are imposed on the factor loadings z. This is because the DFA model is invariant to rotations and reflections of the factor loadings (see Zuur et al., 2003 for details). We impose constraints on the factor loadings by setting the above-diagonal elements of the loading matrix to zero (Harvey, 1990).

Adding more latent trends (i.e. increasing M) will improve the fit of the DFA model. We therefore use AIC to select an optimal number of latent trends (Zuur et al., 2003) and tested different numbers of trends from one to a third of the number of time series (Zimmermann et al., 2019).

DFA models were implemented in Template Model Builder via the R-package TMB (Kristensen et al., 2016). TMB uses Laplace approximations to integrate over random effects. The likelihood function was optimised using the *nlminb* function in R (R Core Team, 2021) and *Nelder–Mead* implemented in the *optim* algorithm, each run three times using three different starting values and selecting the solution with largest log-likelihood.

2.2 | Toolbox

2.2.1 | Tool 1: Visualising latent trends

As the dynamics of species are constructed from linear combinations of latent trends, the estimated latent trends provide information about the general types of dynamics going on among the set of species, and about the diversity of dynamics behind the multi-species index. The first tool is therefore to visualise the latent trends (Griffiths et al., 2020; Zimmermann et al., 2019). Since the DFA model is invariant to rotations of the factor loadings, any choice of rotation could in principle be used for plotting the latent trends. A common and useful choice, which we adopt, is the varimax rotation (Holmes et al., 2014). The purpose of it is to aid interpretation of the rotated latent trends and the corresponding loadings. Intuitively, this

is done by rotating so that the loadings for species are concentrated on as few latent trends as possible (see Jackson, 2005 for technical details behind varimax rotation). We then display the varimax rotated trends. Additionally, the loadings of species on these rotated trends can be plotted. This gives visual and quantitative information about which species are most associated with a specific latent trend and thus gives a first idea of whether some species dynamics deviate from other species in the index group.

2.2.2 | Tool 2: Ordination biplots

The factor loadings of the DFA model determine the contributions of the latent trends to the dynamics of the species, and species with similar factor loadings will have similar dynamics up to random noise captured by $\eta_{i,t}$. The factor loadings can therefore be used as a basis for an ordination of species dynamics (Zuur et al., 2003). For this ordination, factor loadings may be plotted directly if there are less than three latent trends. If the number of latent trends is three or larger, we use a principal component analysis (PCA) of the factor loading matrix to reduce the dimension for plotting. The resulting plot (i.e. the first factorial plane) visualises the distribution of species dynamics in a continuous space formed by coefficients (factor loadings) for the latent trends. It therefore provides an additional clue of whether and how the dynamics of some species deviate from those of the majority of species in the index group.

2.2.3 | Tool 3: *K*-means clustering

The third tool is aimed at objectively detecting potential clusters of species that share similar dynamics. The clusters can then be incorporated visually in the ordination biplots. For the clustering, we use the *k*-means algorithm (although other clustering methods could be considered) of the factor loadings of the species. We estimate an optimal number of species clusters while accounting for the uncertainty in the factor loadings. To do so, we first run a k-means analysis on the point estimates of the factor loadings to obtain a reference partition. We select the number of clusters in the reference partition according to the number most frequently indicated by the 30 indices calculated by the *NbClust* function (Charrad et al., 2014). To incorporate uncertainty of the factor loadings, we then run a bootstrap routine by sampling 500 sets of factor loadings from a multivariate normal distribution with mean equal to the point estimates of the factor loadings obtained from the DFA fit and with a covariance obtained from the Hessian matrix of the model fit, representing variances and covariances among the estimated factor loadings. We then run k-means clustering for each of the sampled sets of factor loadings. This results in 500 partitions of the species into estimated clusters. Clusters from each bootstrap sample are then compared to the most similar cluster in the reference partition using Jaccard similarity following Hennig (2007). The Jaccard similarities J_{kb} between cluster k in the

reference partition and its most similar cluster in bootstrap sample b are then used to calculate $\bar{J}_k$, the cluster *stability*, as the mean Jaccard similarity for cluster k (Equation 3):

$$\bar{J}_k = \frac{1}{B} \sum_{b=1}^{B} J_{kb} \qquad (3)$$

with B the number of bootstrap partitions. Clusters in the reference partition with a high stability will therefore tend to have a corresponding similar cluster in many of the bootstrap samples. In other words, a cluster with high stability will have a species list that will remain fairly stable across bootstrap samples.

If the stability of one of the clusters in the reference partition is below 0.5, we rerun the full clustering procedure with a reference partition reduced by one cluster to dissolve the cluster with low stability (Hennig, 2007).

In addition to the *stability* of clusters, we estimate cluster *dispersion* by calculating the spread of the factor loadings within each cluster. To do so, we first calculate the coordinates of the cluster centre c_c as the mean of the factor loadings of species from this cluster weighted by the specificity of species (i.e. their frequency of attribution to the cluster, using J_{kb} to link the estimated cluster with one of the reference clusters). Cluster *dispersion* D_c was then obtained by averaging the Euclidean distance between the species factor loadings (independently of specificity) and the centre position of the cluster c (Equation 4):

$$D_c = \frac{1}{I_c} \sum_{i_c}^{I_c} \sqrt{\sum_{j}^{M} \left(z_{i_c,j} - c_{cj}\right)^2} \qquad (4)$$

with I_c the number of species in the cluster, M the number of latent trends, $z_{i_c,j}$ the factor loading of species i_c for the latent trend j and c_{cj} the coordinate of the cluster centre c_c for latent trend j.

To visualise the dynamics of a cluster, we use the weighted average of the loadings of the species within the cluster (i.e. the cluster centre above) as loadings for the latent trends to estimate the cluster centre dynamics. When displayed at the arithmetic scale, the resulting dynamics represent a (weighted) geometric mean of the dynamics of the species in the cluster. The uncertainty of the cluster centre dynamics was estimated by fixing factor loadings at the weighted cluster average and using the *sdreport* function from the TMB package to estimate uncertainty, see Kristensen et al. (2016). This will give a crude estimate as uncertainty in cluster membership is only considered via the weighting and cluster centre loadings are held fixed, but we lack a computationally feasible better alternative. Singleton clusters (i.e. with only one species) are not considered as clusters but as outlier species and their stability, dispersion and centre dynamics are not computed.

2.2.4 | R-package

The three tools are implemented in the R package DFACLUST available at https://github.com/StanislasRigal/DFAclust. In this package,

the default format of input data for the function performing DFA (*fit_dfa*) are log-scaled mean-centred time series, but alternatively, time series centred on the first year of data can be provided as input data. In addition, by default *fit_dfa* chooses the optimal number of latent trends (within an interval specified by the user), but the number of latent trends can also be provided by the user.

There is a specific function to prepare data into the suitable format (*prepare_data*). Species time series may contain gaps due to incomplete monitoring (e.g. missing values, zeros and lack of uncertainty data). The likelihood of the DFA is then calculated only over non-missing values, that is omitting the likelihood contributions from the missing data points. Another issue may result from the presence of zeros in time series that would prevent the use of a log-scale index. By default, zeroes are replaced by 1% of the mean of the values of the species time series (but the user can specify another percentage), following common practice used for the LPI and other MSIs (Collen et al., 2009; Soldaat et al., 2017). If the standard error of the indices is not available for some time steps and species, missing values in ε are replaced as follows (Equation 5):

$$\varepsilon_{\text{NA}} = \sqrt{\overline{\varepsilon_i^2}} \qquad (5)$$

with ε_{NA} the missing value in ε and $\overline{\varepsilon_i^2}$ the mean of the squared standard errors over the available values for species i. Finally, if standard errors are not available at all for one or several time series, the ε error term is dropped (i.e. ε is assumed to be equal to zero for those time series) and noise is entirely captured by the $\eta_{i,t}$.

2.3 | Application on Swedish breeding birds

To illustrate the toolbox on real data, we used counts of common breeding birds in Sweden obtained from the Swedish Bird Survey (Lindström & Green, 2021). The survey has been monitoring common and widespread bird species since 1996 on 716 fixed routes, each route consisting of an 8-km line transect. The survey is carried out between 20 May and 5 July each year and consists in counting all birds heard or seen while slowly walking along the transect.

We initially computed annual indices with enough data according to five criteria (Lorrillière & Gonzalez, 2016): (i) more than three consecutive years in which the species was detected (i.e. at least one non-zero count), (ii) less than four consecutive years in which the species was not detected, (iii) at least one detection in the first year, (iv) the median of the number of routes at which the species is detected per year is larger than three, and (v) a median of abundance per year larger than five, among the 107 species used in Wild Bird Indices in Sweden (Svensk fågeltaxerings, 2021). We used data between 1998 and 2020 as the number of routes monitored in 1996 and 1997 was low (Lindström et al., 2007).

For each species, we estimated annual national population indices and their uncertainties. To obtain these annual estimates, we used a quasi-Poisson generalised linear model (GLM) with the following structure (Equation 6):

$$Count \sim QP(exp(Year + Route)), \qquad (6)$$

where Count are the annual site-specific counts of the species and Year and Route are fixed factors. From the fitted models (i.e. those with an overdispersion smaller than 3), we extracted the mean-centred estimate of the year effects (representing a log-scale mean-centred population index; Knape, 2023), and the associated standard errors as inputs to the DFA analysis. We were thus able to estimate the time series and standard errors of 104 of the 107 species, three species being removed from the analysis by the five criteria on data detailed above and the overdispersion criterion on the model fit.

We applied the DFA analysis to (i) the set of 15 farmland bird species used for the official EU-farmland bird indicator for Sweden (Svensk fågeltaxerings, 2021) (see species list in Supporting Information 1) and (ii) the 26 woodland bird species used to produce the EU-woodland bird indicator for Sweden (Svensk fågeltaxerings, 2021) (see species list in Supporting Information 1). Additionally, results for all the 104 common bird species are available in Supporting Information 2.

2.4 | Simulation study

2.4.1 | Simulate latent trends

As the clustering tool goes beyond standard applications of DFA, we focused on this part of the toolbox to explore performance via simulated time series. To do so, we simulated random walk latent trends (Equation 2). We used three latent trends (α_1, α_2 and α_3), 25 time steps and 15 species time series (the same order of magnitude as in European wild bird indicators; Gregory & Van Strien, 2010) to test the influence of the number of clusters and the proximity between clusters on the performance of the clustering tool. From α_1, α_2 and α_3, we simulated C clusters of factor loadings, each cluster containing $n_c = \frac{15}{C}$ (rounded if not an integer and n_c of one cluster adjusted if needed to always keep 15 species) time series.

2.4.2 | Simulate clustered factor loadings

For each species i belonging to a simulated cluster c, the factor loading for each latent trend j was drawn independently from a trivariate normal distribution $N(\mu_{cj}, \varsigma^2 I)$, where I is the identity matrix. In other words, the variance around the cluster centre was the same in all three dimensions and also across all clusters. The means of the factor loadings of the clusters, that is the simulated cluster centres μ_{cj}, were arranged in the three-dimensional space so that the distance d between any two centres was equal (see details in Supporting Information 3). From ς, the standard deviation of the factor loadings within clusters, and d, the distance between cluster centres, we defined the proximity between pair of clusters as $p = \frac{\varsigma}{d}$. This is a scale-free measure of the proximity between the species pool of one

cluster and the species pool of another cluster, which determines the overlap between clusters.

2.4.3 | Simulate time series

The simulated factor loadings, together with the latent trends, determine expected population trajectories for all species. To this, we add two noise components to all trajectories, corresponding to η and ε in Equation (1).

First, we add random white noise to the expected trajectories. The white noise sequences are drawn from a normal distribution $N(0, \tau)$ with the same variance $\tau = 0.05$ for all species. We assume that the variance of this component is unknown (i.e. the value 0.05 is not used when fitting the simulated time series). This noise component corresponds to η in Equation (1).

Second, we simulate noise corresponding to index uncertainty (ε in Equation 1) with a variance that is assumed known and used as input when fitting the model. For this, we again drew independent normally distributed values, but let the variance vary over time and across species. The variance for species j at time t (corresponding to the squared standard error for species j at time t) was simulated as the absolute value of a random variable drawn from a normal distribution with a mean equal to 10% of the range of the species time series simulated via the latent trends and the first noise component (see above), and with a standard deviation equal to 0.01. In this way, the noise (corresponding to ε) and its standard error will be larger for simulated series with a wider range.

2.4.4 | Number of clusters

We first tested for the influence of the number of clusters C, fixing p, the proximity between clusters, to 0.1. We simulated 200 sets of time series for each value of C in [1, 2, 3, 4]. In total, 800 sets of time series were simulated for this test.

2.4.5 | Proximity between clusters

We then tested for the influence of cluster proximity p, fixing the number of clusters C to 2. We simulated 200 sets of time series for each value of p in [0.01, 0.05, 0.1, 0.2, 0.5, 1]. In total, 1200 sets of time series were simulated for this test.

2.4.6 | Fitting models to simulated data

We applied the toolbox to each simulated data set, estimating the optimal number of latent trends (between 1 and 5). To assess to what extent the clustering tool was able to recover the simulated clusters, we finally measured the *stability* of the simulated clusters, and their *similarity* to the true clustering as 1—the Jaccard distance between

clusters in the output of the model compared to the clustering used for simulating the data.

3 | RESULTS

3.1 | Application on Swedish wild bird index

3.1.1 | Farmland bird index

We found three latent trends for the 15 farmland bird species (Figure 1a). The first one, U-shaped, to which most species were positively related, explained at least a third of the variance in dynamics of the Barn swallow *Hirundo rustica*, the Common linnet *Linaria cannabina*, the Rook *Corvus frugilegus* and the Eurasian skylark *Alauda arvensis*. The second one, with a reversal of the dynamics around 2002, explained at least a third of the variance of the Eurasian tree sparrow *Passer montanus* and the Western yellow wagtail *Motacilla flava* dynamics. The third one, with a reversal of

the dynamics around 2007, explained more than half of the variance of the Ortolan bunting *Emberiza hortulana*, the Northern lapwing *Vanellus vanellus* and the European starling *Sturnus vulgaris* dynamics (see factor loadings and computation of variance proportion in Supporting Information 2).

In the ordination biplot (representing the first factorial plane of the PCA on the three latent trends, Figure 2a), the Ortolan bunting, a species that has undergone a sharp decline in the last few decades, is visually isolated from the rest of the species along the first PCA axis which explains most of the existing variation (43.9%). The other species are mainly segregated along the second axis (capturing 34.6% of the variation) with meadow pipit *Anthus pratensis* and the Common kestrel *Falco tinnunculus* at opposing ends.

The clustering tool confirms the visually observed position of the Ortolan bunting as an outlier species and furthermore indicates that the 14 remaining farmland bird species were separated into two clusters (Figure 2a): one cluster of 11 species (*stability*, i.e. cluster similarity across bootstraps = 0.69) and one other cluster of three species (*stability* = 0.51). The dispersion of the first cluster is slightly
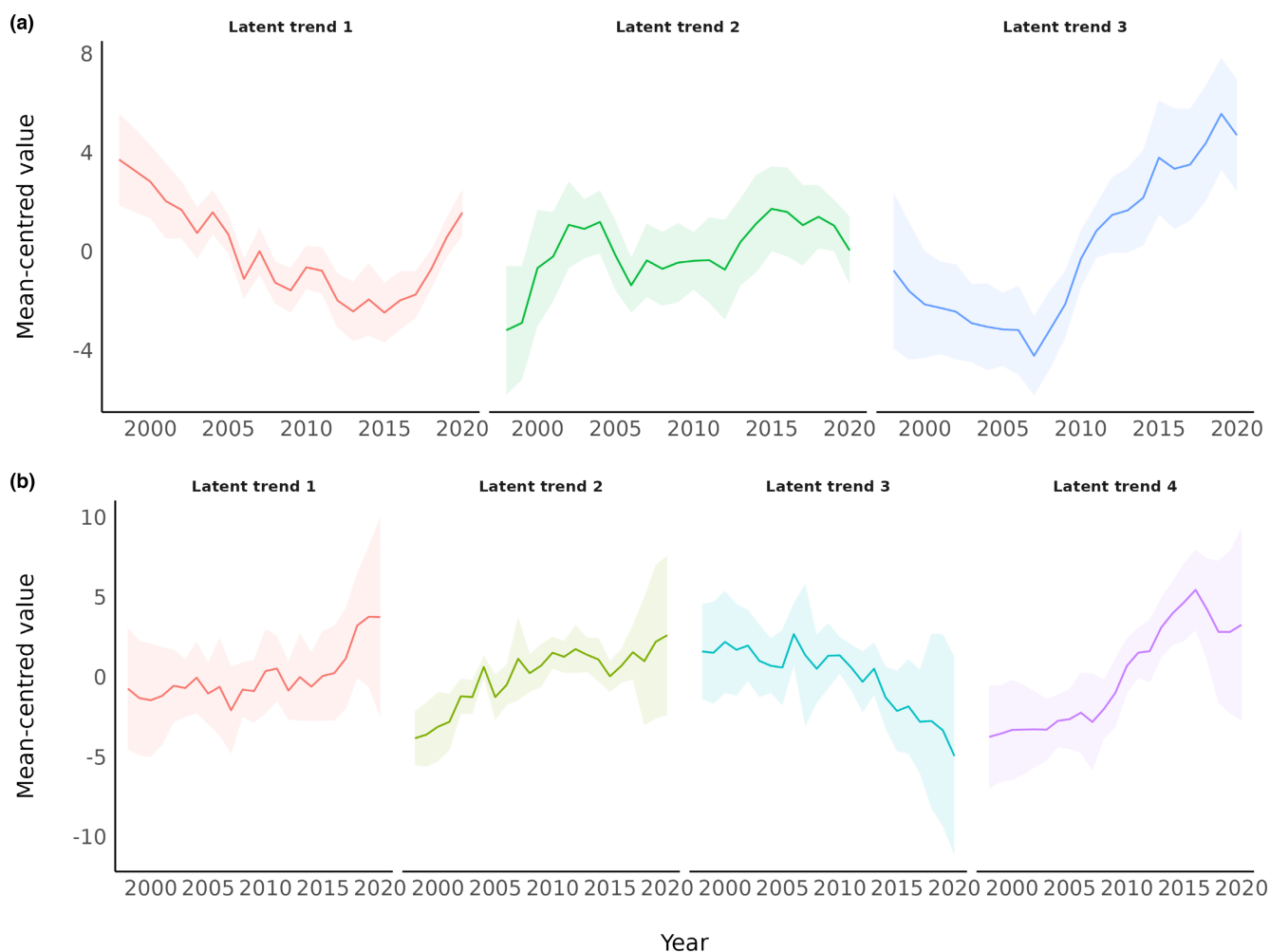
FIGURE 1 Latent trends from the dynamic factor analysis (DFA) model. (a) The three latent trends obtained for the 15 farmland species and (b) the four latent trends obtained for the 26 woodland species. The shaded areas correspond to the 95% confidence intervals.
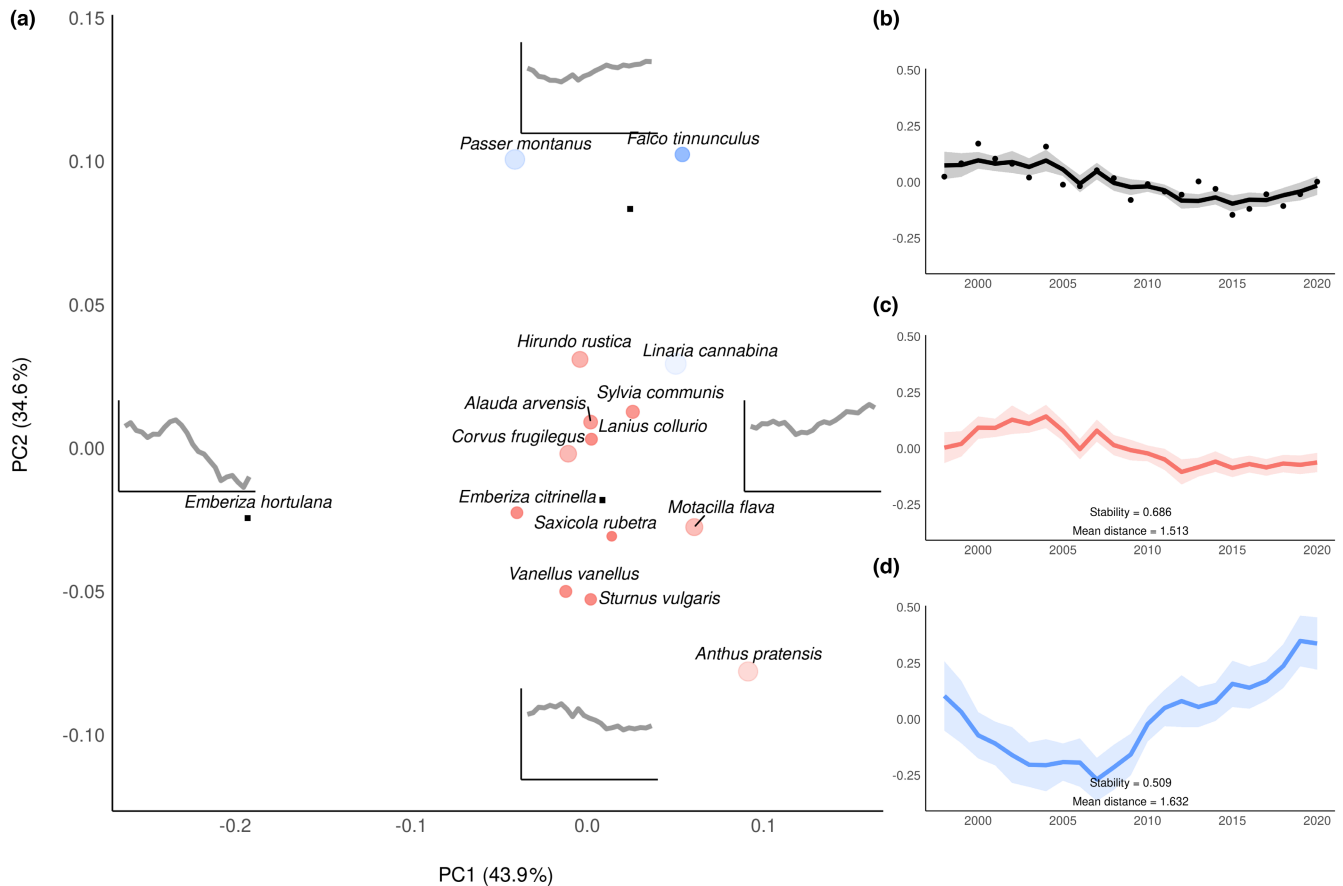
FIGURE 2 Heterogeneity in species dynamics among Swedish farmland birds ($n=15$). (a) Clusters of species displayed in the first factorial plane obtained from a PCA on the factor loadings (three latent trends). Species of each cluster are shown by different colours (cluster 1: 11 species in red, cluster 2: three species in blue and one species (the Ortolan bunting, *Emberiza hortulana*) out of the two clusters). Cluster centres are shown by black square dots. Species stability into a cluster is shown by the size and the brightness of its dot: species always associated with one cluster are depicted by small and bright dots. Insert plots show the variation in dynamics along the first and second principal component axes with remaining loadings set to 0. (b) Multi-species index of the 15 farmland species between 1998 and 2020 obtained from the latent trends and the means of all the factor loadings (line), and geometric means of species abundances (dots). (c) Time series of the centre of the first cluster between 1998 and 2020. Approximate standard errors are shown by the shaded area. Cluster stability = 0.69 and scaled mean distance between species and cluster centre = 1.51. (d) Time series of the centre of the second cluster between 1998 and 2020. Standard error shown by the shaded area. Cluster stability = 0.51 and scaled mean distance between species and cluster centre = 1.63. All trends are shown at the log scale.

smaller (mean distance = 1.51) than that of the second (mean distance = 1.63). The time series of the centre of the first cluster has overall been decreasing between 1998 and 2020 (*slope* = −0.009, SD = 0.002) with an initial increase followed by a later decline (Figure 2c) which is visible in the species that compose it (eight decreasing, one increasing, two with uncertain direction, see details on species slopes in Supporting Information 2). The time series of the centre of the first cluster shows a strong correlation with the trend from the means of all the factor loadings ($\rho_{Pearson}=0.93$, Figure 2b,c). Despite an initial decline, the time series of the centre of the second cluster has increased overall between 1998 and 2020 (*slope* = 0.019, SD = 0.004, two species with uncertain direction, one increasing, see details on linear species slopes in Supporting Information 2) and is negatively correlated to the trend from the means of all the factor loadings ($\rho_{Pearson}=-0.59$, Figure 2b,d).

3.1.2 | Woodland birds index

Four latent trends were found for the 26 woodland bird species (Figure 1b). The first had a minimum (resulting in a peak for species with negative loadings) in 2007 and explained at least half of the variance of the Willow tit *Poecile montanus*, the Lesser spotted woodpecker *Dryobates minor* and the Marsh tit *Poecile palustris* dynamics. The second was monotonous and explained three quarters of the variance of the Mistle thrush *Turdus viscivorus* and the Rustic bunting *Emberiza rustica* dynamics. The third had a change in the dynamics around 2010 with a monotonous decline after this date. Most species were negatively related to this trend, which explained at least half of the variance of the Goldcrest *Regulus regulus* and the Eurasian treecreeper *Certhia familiaris* dynamics. The fourth had an abrupt change around 2016 and explained most of the variance of

the Hawfinch *Coccothraustes coccothraustes* dynamics (see factor loadings in Supporting Information 2).

The 26 woodland bird species were separated into two clusters (Figure 3a): one cluster of 6 species (*stability* = 0.69) and one cluster of 20 species (*stability* = 0.74) with the first cluster slightly more dispersed (*mean distance* = 1.78) than the second (*mean distance* = 1.70). The time series of the centre of the first cluster has erratic dynamics with an overall increase between 1998 and 2020 (*slope* = 0.012, SD = 0.004) and was correlated with the trend from the means of all the factor loadings ($\rho_{Pearson}$ = 0.93, Figure 3b,c). Most of the species belonging to this cluster have also increased (one decreasing, two with uncertain direction, three increasing, see Supporting Information 2). The time series of the centre of the second cluster also shows an increase between 1998 and 2020, which is more consistent than for the first cluster (*slope* = 0.011, SD = 0.001). Most of the species are increasing (three decreasing, six with uncertain direction and 11 increasing, see Supporting Information 2) and the

cluster centre time series is similarly correlated to the trend from the means of all the factor loadings ($\rho_{Pearson}$ = 0.91, Figure 3b,d). Species from the second cluster are mostly positively related to the first and fourth latent trends and negatively to the third latent trend. Species from the first cluster are mainly positively related to the second latent trend.

3.2 | Simulation results

3.2.1 | Sensitivity of clustering to the number of clusters

Overall, the clustering tool is providing clusters very similar to the simulated clusters, in particular when there are between one and three simulated clusters (Table 1). When there are more than two clusters, the clustering tends to be conservative and underestimate
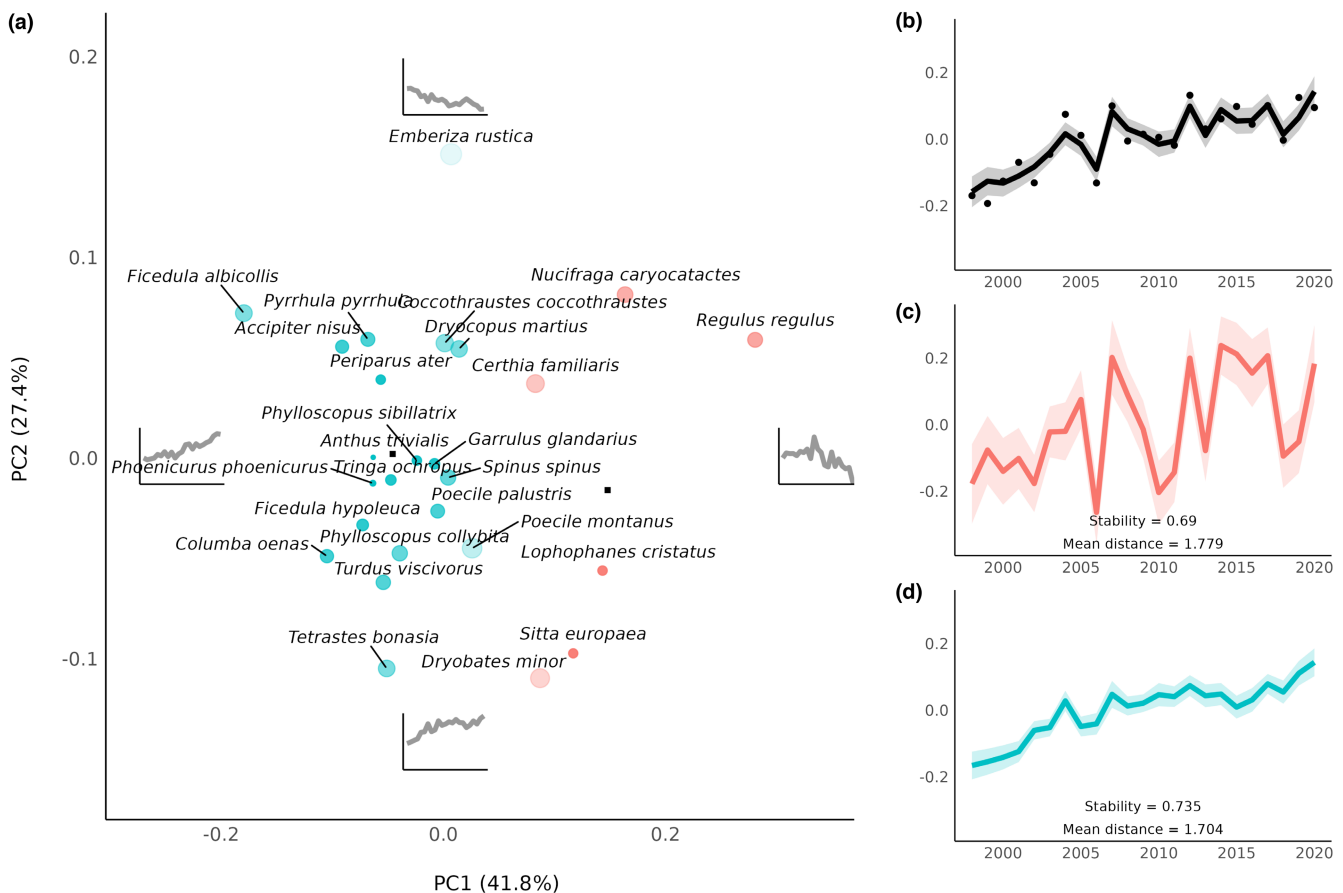
FIGURE 3 Heterogeneity in species dynamics among Swedish woodland birds (*n* = 26). (a) Clusters of species displayed in the first factorial plane obtained from a PCA on the factor loadings (four latent trends). Species of each cluster are shown in a different colour (cluster 1: 6 species in red, cluster 2: 20 species in blue). Cluster centres are shown by black square dots. Species stability into a cluster is shown by the size and the brightness of its dot: species always associated with one cluster are depicted by small and bright dots. (b) Multi-species index of the 26 woodland species between 1998 and 2020 obtained from the latent trends and the means of all the factor loadings (line), and geometric means of species abundances (dots). (c) Time series of the centre of the first cluster between 1998 and 2020. Approximate standard error is shown by the shaded area. Cluster stability = 0.69 and scaled mean distance between species and cluster centre = 1.78. (d) Time series of the centre of the second cluster between 1998 and 2020. Standard error is shown by the shaded area. Cluster stability = 0.74 and scaled mean distance between species and cluster centre = 1.70. All trends are shown at the log scale.

the number of clusters rather than overestimate it (Table 2). In addition to the similarity with simulated clusters, estimated clusters are also highly stable in this simulation (Table 1) (a threshold of 0.7 has been proposed to define high cluster stability; Hennig, 2007).

3.2.2 | Cluster proximity

In the test of the influence of cluster proximity, estimated clusters remain very similar to simulated clusters while the proximity stays below 0.5 (Table 3). The similarity between simulated and estimated clusters decreases above 0.5 as the clusters are less and less separated (Table 3 and see example in Supporting Information 3). Cluster stability remains high over the whole range of tested proximity. It also starts to decrease above a proximity of 0.5 (Table 3) as the clusters are less and less separated.

4 | DISCUSSION

We present a toolbox for systematically investigating the diversity of species dynamics underlying aggregated biodiversity indices. The toolbox is based on identifying latent trends among species time series through DFA (Zuur et al., 2003), accounting for observation error, to explore the variability of species time series and identify potential clusters displaying a similar pattern of dynamics. It can be

used to complement biodiversity aggregate index interpretation and highlight possible challenges in current conservation strategies for the index species as a group (Leung et al., 2020).

To demonstrate the method, we applied it to empirical data on Swedish common birds. The MSI of farmland birds shows a general decline in recent decades in Sweden (Svensk fågeltaxerings, 2021; Wretenberg et al., 2006) and similar declines have been reported elsewhere in Europe (Donald et al., 2001; Voříšek et al., 2010). Our tool suggested that the decline of farmland birds in Sweden is driven by one cluster of species that have experienced declining dynamics since the beginning of the century, with a potential stabilisation in the last few years (Figure 2c). However, one other cluster consists of species that have not decreased or have even increased since 1998 (Figure 2d). This latter cluster is partly responsible for the deceleration of the decline and the late increase visible in the MSI between 2015 and 2020. One species (the Ortolan bunting) does not belong to any clusters as its steep decline makes its time series singular and deviating strongly from the others. Although it is well known that population dynamics for farmland birds display variable pattern among species dynamics (Voříšek et al., 2010; Wretenberg et al., 2006), farmland birds have often been discussed or analysed as a group of species (Donald et al., 2001; Reif & Vermouzek, 2019; but see Gaüzère et al., 2019; Stjernman et al., 2013). Assessing the mechanisms explaining these differences among farmland birds will necessitate more studies, but our three tools provides new insights into how

TABLE 1 Influence of the numbers of clusters on the similarity between estimated clusters and simulated clusters and the stability of estimated clusters.

Number of simulated clusters	1	2	3	4
Mean of similarity	0.92	0.98	0.95	0.92
Standard deviation of similarity	0.16	0.07	0.10	0.11
Mean of cluster stability	0.93	0.97	0.93	0.88
Standard deviation of cluster stability	0.14	0.07	0.07	0.07

TABLE 2 Contingency table between the number of estimated clusters (rows) and the number of true simulated clusters (columns) with percentage of the number of simulations. Estimated clusters composed of only one species have not been considered in the number of estimated clusters.

Number of clusters	1	2	3	4
1	162 (81.0%)	5 (2.5%)	0	0
2	12 (6.0%)	189 (94.5%)	40 (20.0%)	24 (12.0%)
3	23 (11.5%)	4 (2.0%)	156 (78.0%)	58 (29.0%)
4	3 (1.5%)	2 (1.0%)	4 (2.0%)	118 (59.0%)

TABLE 3 Influence of cluster proximity on the similarity between estimated clusters and simulated clusters and the stability of estimated clusters. The cluster proximity corresponds to the ratio between the standard deviation of the factor loadings and the minimum distance between centres of clusters.

Cluster proximity	0.01	0.05	0.1	0.2	0.5	1
Mean of similarity	0.99	0.99	0.98	0.92	0.74	0.69
Standard deviation of similarity	0.07	0.06	0.07	0.11	0.12	0.11
Mean of cluster stability	0.99	0.99	0.97	0.85	0.75	0.75
Standard deviation of cluster stability	0.02	0.03	0.07	0.11	0.10	0.09

the dynamics within the group of species are structured and opens up for finding common denominators for the groups.

In contrast to farmland birds, the MSI of woodland birds has increased over the past two decades (Figure 3b; Ram et al., 2017; Svensk fågeltaxerings, 2021). Two clusters were revealed: one composed of mainly increasing species (Figure 3d) and the other group of species showing a greater yearly variability in the late 2000s (Figure 3c). The latter cluster was only composed of non-migratory species with a high proportion of small-bodied species (in particular the Eurasian nuthatch *Sitta europaea*, the Goldcrest, the Eurasian treecreeper and the European crested tit *Lophophanes cristatus*) (Storchová & Hořák, 2018). Although the other group contains a few species with similar characteristics, small resident species can be expected to be more strongly affected by harsh winter conditions and thus show higher annual variation (Gregory et al., 2007). Therefore, the overall increase visible in the woodland aggregated index encompasses at least two different types of dynamics and our toolbox highlights species that deviate from this increase, providing clues for the conservation of woodland biodiversity.

The toolbox is aimed at geometric mean biodiversity indices, and the accompanying R package can handle missing values in species time-series, zero indices can be dealt with using common practice procedures for MSIs. It can also be used when uncertainty estimates of the indices are lacking. In the setup of our simulations, the toolbox was able to reasonably recover the true structure of the data. However, it will be useful mainly for indices built from a moderate number of species with fairly complete time series. A large number of species or many gaps in the data can lead to convergence issues or not very informative results (e.g. high number of latent trends and no distinguishable clusters). This turned out to be the case when using the method on 104 species which suggested a wide range of dynamics going on in the system (many latent trends) and no clear clusters were identified (see Supporting Information 2). We rather suggest to use the toolbox for indices with a reasonable number of species (e.g. up to 50, but this may be context dependent) which already encompass a wide range of geometric mean indices used in practice.

5 | CONCLUSIONS

Although the variability of biodiversity dynamics is widely recognised, it remains challenging to understand its consequences for aggregate biodiversity indices whose simplicity contributes to its use in the political sphere (Weber et al., 2004). Our toolbox opens up for thoroughly investigating the precision of present species indices as an indicator of ecosystem health and aid the interpretation of aggregated species indices by recognising the existence of clusters of species with different and even opposite dynamics. It could also be used in the development of new indicators based on existing species time series data, by assessing whether a particular set of species selected to target some aspect of biodiversity of interest display coherent dynamics. If the empirical example focus on species indices,

the toolbox is not restricted to the analysis of such indices, but can be used on other sets of multivariate time series. In general, it enables an analysis on the variable temporal changes going on within communities and may help to refine our understanding of variability in biodiversity dynamics, which is essential for effective conservation policies.

AUTHOR CONTRIBUTIONS

Stanislas Rigal and Jonas Knape conceived the ideas and designed the methodology. Stanislas Rigal analysed the data and led the writing of the manuscript. Jonas Knape contributed critically to the drafts and gave final approval for publication.

CONFLICT OF INTEREST STATEMENT

The authors have no conflict of interest to declare.

PEER REVIEW

The peer review history for this article is available at https://www.webofscience.com/api/gateway/wos/peer-review/10.1111/2041-210X.14117.

DATA AVAILABILITY STATEMENT

All the analyses were conducted in R 4.1.2 (R Core Team, 2021). A R package with ready-to-use functions is available on Github (Rigal & Knape, 2023) with a detail of functions and data used (available in Lindström & Green, 2021), and a reproducible example is available in the R package VIGNETTE.

ORCID

Stanislas Rigal 🔟 https://orcid.org/0000-0002-3180-4592
Jonas Knape 🔟 https://orcid.org/0000-0002-8012-5131

REFERENCES

Buckland, S. T., Magurran, A. E., Green, R. E., & Fewster, R. M. (2005). Monitoring change in biodiversity through composite indices. *Philosophical Transactions of the Royal Society, B: Biological Sciences*, *360*(1454), 243–254. https://doi.org/10.1098/rstb.2004.1589

Charrad, M., Ghazzali, N., Boiteau, V., & Niknafs, A. (2014). NbClust: An R package for determining the relevant number of clusters in a data set. *Journal of Statistical Software*, *61*, 1–36. https://doi.org/10.18637/jss.v061.i06

Collen, B., Loh, J., Whitmee, S., McRAE, L., Amin, R., & Baillie, J. E. M. (2009). Monitoring change in vertebrate abundance: The living planet index. *Conservation Biology*, *23*(2), 317–327. https://doi.org/10.1111/j.1523-1739.2008.01117.x

Costelloe, B., Collen, B., Milner-Gulland, E. J., Craigie, I. D., McRae, L., Rondinini, C., & Nicholson, E. (2016). Global biodiversity indicators reflect the modeled impacts of protected area policy change. *Conservation Letters*, *9*(1), 14–20. https://doi.org/10.1111/conl.12163

Donald, P. F., Green, R. E., & Heath, M. F. (2001). Agricultural intensification and the collapse of Europe's farmland bird populations. *Proceedings of the Royal Society of London. Series B: Biological Sciences*, *268*(1462), 25–29. https://doi.org/10.1098/rspb.2000.1325

EEA. (2019). *The European environment—State and outlook 2020—European Environment Agency* [publication]. European Environment Agency. https://www.eea.europa.eu/ds_resolveuid/301fc55a26a943bc8de1cd5d17d7ec66

Freeman, S. N., Baillie, S. R., & Gregory, R. D. (2001). *Statistical analysis of an indicator of population trends in farmland birds*. BTO Research Report.

Gaüzère, P., Doulcier, G., Devictor, V., & Kéfi, S. (2019). A framework for estimating species-specific contributions to community indicators. *Ecological Indicators*, *99*, 74–82. https://doi.org/10.1016/j.ecolind.2018.11.069

Gregory, R. D., Noble, D., Field, R., Marchant, J., Raven, M., & Gibbons, D. W. (2003). Using birds as indicators of biodiversity. *Ornis Hungarica*, *12*(13), 11–24.

Gregory, R. D., & Van Strien, A. (2010). Wild bird indicators: Using composite population trends of birds as measures of environmental health. *Ornithological Science*, *9*(1), 3–22. https://doi.org/10.2326/osj.9.3

Gregory, R. D., Vorisek, P., Van Strien, A., Gmelig Meyling, A. W., Jiguet, F., Fornasari, L., Reif, J., Chylarecki, P., & Burfield, I. J. (2007). Population trends of widespread woodland birds in Europe. *Ibis*, *149*, 78–97. https://doi.org/10.1111/j.1474-919X.2007.00698.x

Griffiths, J. R., Lehtinen, S., Suikkanen, S., & Winder, M. (2020). Limited evidence for common interannual trends in Baltic Sea summer phytoplankton biomass. *PLoS ONE*, *15*(4), e0231690. https://doi.org/10.1371/journal.pone.0231690

Harvey, A. C. (1990). *Forecasting, structural time series models and the Kalman filter*. Cambridge University Press.

Hennig, C. (2007). Cluster-wise assessment of cluster stability. *Computational Statistics & Data Analysis*, *52*(1), 258–271. https://doi.org/10.1016/j.csda.2006.11.025

Holmes, E. E., Ward, E. J., & Kellie, W. (2012). MARSS: Multivariate autoregressive state-space models for analyzing time-series data. *The R Journal*, *4*(1), 11. https://doi.org/10.32614/RJ-2012-002

Holmes, E. E., Ward, E. J., & Scheuerell, M. D. (2014). Analysis of multivariate time-series using the MARSS package. *NOAA Fisheries, Northwest Fisheries Science Center*, *2725*, 98112. https://doi.org/10.5281/zenodo.5781847

Inger, R., Gregory, R., Duffy, J. P., Stott, I., Voříšek, P., & Gaston, K. J. (2015). Common European birds are declining rapidly while less abundant species' numbers are rising. *Ecology Letters*, *18*(1), 28–36. https://doi.org/10.1111/ele.12387

Jackson, J. E. (2005). Varimax rotation. In *Encyclopedia of biostatistics*. John Wiley & Sons, Ltd. https://doi.org/10.1002/0470011815.b2a13091

Julliard, R., Jiguet, F., & Couvet, D. (2004). Common birds facing global changes: What makes a species at risk? *Global Change Biology*, *10*(1), 148–154. https://doi.org/10.1111/j.1365-2486.2003.00723.x

Keith, D., Akçakaya, H. R., Butchart, S. H., Collen, B., Dulvy, N. K., Holmes, E. E., Hutchings, J. A., Keinath, D., Schwartz, M. K., & Shelton, A. O. (2015). Temporal correlations in population trends: Conservation implications from time-series analysis of diverse animal taxa. *Biological Conservation*, *192*, 247–257. https://doi.org/10.1016/j.biocon.2015.09.021

Knape, J. (2023). Effects of choice of baseline on the uncertainty of population and biodiversity indices. *Environmental and Ecological Statistics*, *30*(1), 1–16. https://doi.org/10.1007/s10651-022-00550-7

Kristensen, K., Nielsen, A., Berg, C. W., Skaug, H., & Bell, B. M. (2016). TMB: Automatic differentiation and Laplace approximation. *Journal of Statistical Software*, *70*, 1–21. https://doi.org/10.18637/jss.v070.i05

Leung, B., Hargreaves, A. L., Greenberg, D. A., McGill, B., Dornelas, M., & Freeman, R. (2020). Clustered versus catastrophic global vertebrate declines. *Nature*, *588*(7837), 267–271. https://doi.org/10.1038/s41586-020-2920-6

Lin, Y.-J., Roa-Ureta, R. H., Basali, A. U., Alcaria, J. F. A., Lindo, R., Qurban, M. A., Prihartato, P. K., Qasem, A., & Rabaoui, L. (2021). Coarser taxonomic resolutions are informative in revealing fish community abundance trends for the world's warmest coral reefs. *Coral Reefs*, *40*(6), 1741–1756. https://doi.org/10.1007/s00338-021-02181-z

Lindström, Å., & Green, M. (2021). *Swedish Bird Survey: Fixed routes (Standardrutterna). Version 1.12. Department of Biology, Lund University. Sampling event dataset accessed via GBIF.org*. Sveriges Ornitologiska Förening. https://doi.org/10.15468/hd6w0r

Lindström, Å., Svensson, S., Green, M., & Ottvall, R. (2007). Distribution and population changes of two subspecies of chiffchaff Phylloscopus collybita in Sweden. *Ornis Svecica*, *17*(3–4), 137–147. https://doi.org/10.34080/os.v17.22684

Loh, J., Green, R. E., Ricketts, T., Lamoreux, J., Jenkins, M., Kapos, V., & Randers, J. (2005). The living planet index: Using species population time series to track trends in biodiversity. *Philosophical Transactions of the Royal Society, B: Biological Sciences*, *360*(1454), 289–295. https://doi.org/10.1098/rstb.2004.1584

Loreau, M., Cardinale, B. J., Isbell, F., Newbold, T., O'Connor, M. I., & de Mazancourt, C. (2022). Do not downplay biodiversity loss. *Nature*, *601*(7894), E27–E28. https://doi.org/10.1038/s41586-021-04179-7

Lorrillière, R., & Gonzalez, D. (2016). *Déclinaison régionale des indicateurs issus du Suivi Temporel des Oiseaux Communs (STOC)*. Report, Museum national d'Histoire naturelle. https://naturefrance.fr/sites/default/files/202008/160513_note_methodologique_indice_stoc.pdf

R Core Team. (2021). *R: A language and environment for statistical computing*. R Foundation for Statistical Computing. https://www.R-project.org

Ram, D., Axelsson, A.-L., Green, M., Smith, H. G., & Lindström, Å. (2017). What drives current population trends in forest birds–forest quantity, quality or climate? A large-scale analysis from northern Europe. *Forest Ecology and Management*, *385*, 177–188. https://doi.org/10.1016/j.foreco.2016.11.013

Reif, J., & Vermouzek, Z. (2019). Collapse of farmland bird populations in an eastern European country following its EU accession. *Conservation Letters*, *12*(1), e12585. https://doi.org/10.1111/conl.12585

Rigal, S., & Knape, J. (2023). *DFAclust package v.1.0.0*. https://doi.org/10.5281/zenodo.7828154. https://github.com/StanislasRigal/DFAclust

Soldaat, L. L., Pannekoek, J., Verweij, R. J. T., van Turnhout, C. A. M., & van Strien, A. J. (2017). A Monte Carlo method to account for sampling error in multi-species indicators. *Ecological Indicators*, *81*, 340–347. https://doi.org/10.1016/j.ecolind.2017.05.033

Stjernman, M., Green, M., Lindström, Å., Olsson, O., Ottvall, R., & Smith, H. G. (2013). Habitat-specific bird trends and their effect on the farmland bird index. *Ecological Indicators*, *24*, 382–391. https://doi.org/10.1016/j.ecolind.2012.07.016

Storchová, L., & Hořák, D. (2018). Life-history characteristics of European birds. *Global Ecology and Biogeography*, *27*(4), 400–406. https://doi.org/10.1111/geb.12709

Svensk fågeltaxerings. (2021). *Svenska fågelindikatorer*. http://www.fageltaxering.lu.se/sites/default/files/files/svenska_fagelindikatorer_2021.pdf

Van Swaay, C. A., Dennis, E. B., Schmucki, R., Sevilleja, C., Balalaikins, M., Botham, M., Bourn, N., Brereton, T., Cancela, J. P., & Carlisle, B. (2019). *The EU Butterfly Indicator for Grassland species: 1990–2017*. Technical report 23.

Voříšek, P., Jiguet, F., van Strien, A., Škorpilová, J., Klvaňová, A., & Gregory, R. D. (2010). Trends in abundance and biomass of widespread European farmland birds: How much have we lost. *BOU Proceedings–Lowland Farmland Birds III*, *24*.

Ward, E. J., Anderson, S. C., Hunsicker, M. E., & Litzow, M. A. (2022). Smoothed dynamic factor analysis for identifying trends in multivariate time series. *Methods in Ecology and Evolution*, *13*(4), 908–918. https://doi.org/10.1111/2041-210X.13788

Weber, D., Hintermann, U., & Zangger, A. (2004). Scale and trends in species richness: Considerations for monitoring biological diversity for political purposes. *Global Ecology and Biogeography*, *13*(2), 97–104. https://doi.org/10.1111/j.1466-882X.2004.00078.x

Wretenberg, J., Lindström, Å., Svensson, S., Thierfelder, T., & Pärt, T. (2006). Population trends of farmland birds in Sweden and England: Similar trends but different patterns of agricultural intensification. *Journal of Applied Ecology*, *43*(6), 1110–1120. https://doi.org/10.1111/j.1365-2664.2006.01216.x

Zimmermann, F., Claireaux, M., & Enberg, K. (2019). Common trends in recruitment dynamics of north-East Atlantic fish stocks and their links to environment, ecology and management. *Fish and Fisheries*, *20*(3), 518–536. https://doi.org/10.1111/faf.12360

Zuur, A. F., Tuck, I. D., & Bailey, N. (2003). Dynamic factor analysis to estimate common trends in fisheries time series. *Canadian Journal of Fisheries and Aquatic Sciences*, *60*(5), 542–552. https://doi.org/10.1139/f03-030

SUPPORTING INFORMATION

Additional supporting information can be found online in the Supporting Information section at the end of this article.

Data S1. Supporting information including lists of species used in the analyses, additional results produced by the DFAclust software for farmland birds, woodland birds and all common breeding birds in Sweden, and details of the sensitivity analysis.